PHYSICAL REVIEW B **71**, 245415 (2005)

Structure-dependent ferroelectricity of niobium clusters (Nb_N, N=2–52)

Wei Fa, Chuanfu Luo, and Jinming Dong*

Group of Computational Condensed Matter Physics, National Laboratory of Solid State Microstructures, and Department of Physics, Nanjing University, Nanjing 210093, People's Republic of China

(Received 5 April 2005; revised manuscript received 25 April 2005; published 27 June 2005)

The ground-state structures and ferroelectric properties of Nb_N (N=2–52) have been investigated by a combination of density-functional theory in the generalized gradient approximation and an unbiased global search with the guided simulated annealing. It is found that the electric dipole moment (EDM) exists in most of the Nb_N and varies considerably with their sizes. The larger Nb_N ($N \geqslant 25$) prefer the amorphous packing. Most importantly, our numerical EDM values of Nb_N ($N \geqslant 38$) exhibit an extraordinary even-odd oscillation, which is consistent with the experimental observation, showing a close relationship with the geometrical structures of Nb_N. Finally, an inverse coordination number function is proposed to account for the structural relation of the EDM values, especially their even-odd oscillations starting from Nb_{38}.

DOI: 10.1103/PhysRevB.71.245415 PACS number(s): 36.40.Mr, 31.15.Ar, 36.90.+f, 73.22.−f

I. INTRODUCTION

Transition-metal clusters have long been of considerable interest due to their importance in fundamental research and their tremendous potential technical applications, among which the niobium cluster is one of the most thoroughly studied for both its chemical and physical properties. Even so, the full understanding of their dramatic size-dependent properties is still a great challenge. Recently, the ferroelectricity (FE) in free niobium clusters (Nb_N, N=2–150) has been experimentally found at low temperatures,[1,2] showing the existence of electric dipole moments (EDMs), which, more importantly, exhibit a pronounced even-odd oscillation for Nb_N ($N \geqslant 38$). Such an interesting phenomenon has attracted immediate attention because the FE has never been found in single-element bulk materials or in metals. For example, a purely electronic mechanism has been proposed, considering the FE of Nb_N to be caused by the electron correlations.[3] However, the large size-dependent EDMs, especially the remarkable even-odd oscillation starting from N=38, strongly support the existence of an intimate relation between the FE and structures of Nb_N. Since the existing techniques cannot conclusively determine the geometrical structures of clusters, the numerical simulation on them becomes a useful method to provide more valuable information on their structures and novel physical properties.

Several first-principles calculations on Nb_N up to 23 atoms have been performed.[4–6] It was concluded that the icosahedral growth is not favored for Nb_N.[6] Other studies made on the smaller Nb_N ($N \leqslant 10$) found similar lowest-energy structures with the high coordinated configurations. Recently, a close relationship between the asymmetrical geometrical structures of Nb_N ($N \leqslant 15$) and their EDMs has been revealed through a first-principles study.[7] However, there has been no density-functional theory (DFT) study on the larger Nb_N and their ferroelectric properties.

Therefore, in this paper, we will address the growth pattern of Nb_N ($N \leqslant 52$) and its close relation with cluster FE. The relevant structures of Nb_N are obtained by an empirical global optimization combined with the DFT relaxation, from which the EDMs are then calculated by the DFT. The details of the calculated methods are described in Sec. II. The structural and ferroelectric properties of Nb_N are presented in Sec. III. Section IV contains concluding remarks.

II. COMPUTATIONAL METHOD

Instead of the presumed symmetry constraints, an unbiased global search on the potential energy surface of clusters is preformed by the guided simulated annealing (GSA) method,[8,9] which incorporates a guiding function (GF) in the traditional simulated annealing to find the global energy minimum. In our calculations, the density of atoms and the second moment of the mass distribution[10] are adopted as the GFs. The interaction between Nb atoms is represented by an empirical many-body potential,[11,12] which has been successfully applied to predict the equilibrium geometries of Nb_N ($N \leqslant 14$).[13] A number of lower-energy isomers are thereby generated, representing different local stable states in the phase space.

Then, the DMOL3 package[14] based on DFT is used to further optimize the cluster structures by selecting at least five isomers with different symmetries for a given size from the above step, in which a relativistic effective core potential (RECP)[15,16] and a double numerical basis including a *d*-polarization function are chosen to do the electronic structure calculations. The RECP was generated by fitting all-electron Hartree-Fock results, which have been included in the DMol3 package as a powerful method of treating the core electrons. The density functional is treated in the generalized gradient approximation (GGA) with spin polarization, and Perdew and Wang exchange-correlation function is used.[17] Geometrical structure optimization is performed with the Broyden-Fletcher-Goldfarb-Shanno algorithm.[18] A convergence criterion of 10^{-3} a.u. on the gradient and displacement, and 10^{-5} a.u. on the total energy, is used in the optimization. The accuracy of the current computational scheme has been checked by benchmark calculations on the Nb atom and its bulk solid.[19] In addition, a comparison has been made on the results of Nb_N (N=2–19, 43–45) obtained by both

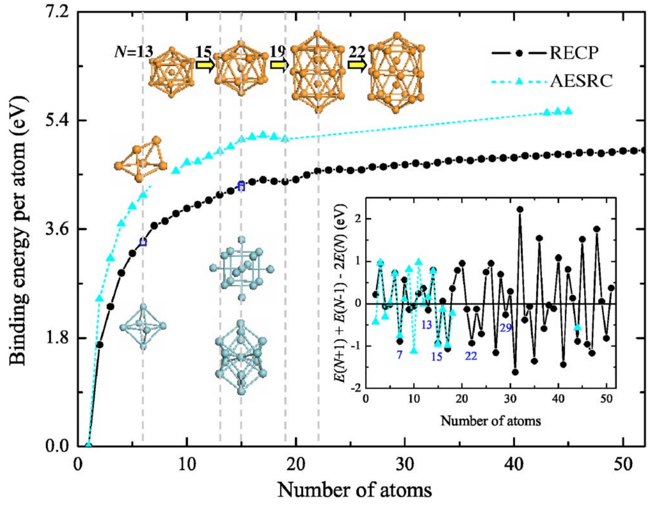

FIG. 1. (Color online) The binding energy (BE) per atom of Nb_N vs cluster size. The inset is the size-dependent second-order difference of BE. The RECP and AESRC results are shown by circles and triangles, respectively. The vertical dashed lines represent the positions at $N=6$, 13, 15, 19, and 22. Geometrical structures of the different isomers for Nb_6 and Nb_{15} are also shown in the order of their BE values from top to bottom. The structural transitions are illustrated by the ground-state structures of Nb_{13}, Nb_{15}, Nb_{19}, and Nb_{22}.

RECP and all-electron calculations with scalar relativistic corrections (AESRC), showing a reasonable consistency between them in predicting the structural order and corresponding properties of Nb_N clusters. With this strategy, we have optimized the equilibrium structures of Nb_N up to 52 atoms in a reliable and efficient way, though we cannot strictly rule out other energetically more favorable structures.

III. RESULTS

The calculated binding energies (BEs) per atom are shown in Fig. 1, in which the isomers and the ground-state structures of some clusters are also included. For small Nb_N ($N=2$–12),[20] our lowest-energy configurations and isomeric order are similar to those found in Ref. 6 except for Nb_8, which has several competitive isomers, such as a capped distorted pentagonal bipyramid and a C_{2v} capped octahedron, within an energy interval of 0.1 eV. Though the atomic packing of the small clusters is gradually changed from one size to another, there exist several structural transitions for medium-sized clusters of $N=13$–24, e.g., from the icosahedron to the icositetrahedron, as illustrated in Fig. 1. Nb_{13} is a distorted icosahedron. By adding one atom to Nb_{13}, one planar pentagon in it will be changed into the first hexagonal ring, forming the structure of Nb_{14}. Again, one more atom causes the opposite planar pentagon in Nb_{14} to become the second hexagonal ring, leading to the equilibrium icositetrahedral structure of Nb_{15}, which is about 0.26 eV and 0.89 eV lower in energy than the distorted bulk bcc type structures with approximate O_h and D_{2h} symmetries, respectively (see Fig. 1). The structures of Nb_{16}–Nb_{18} are obtained by adding one, two, and three bottom atoms to Nb_{15}, holding still the two hexagonal rings (distorted). Nb_{19} is a double icosahedral structure with two core atoms. From Nb_{20} to Nb_{22}, the structures evolve into a slightly distorted double-interpenetrating icositetrahedron with three parallel hexagonal rings, which are obtained by adding one, two, and three atoms to the three pentagons of Nb_{19}, respectively. Nb_{23} is formed by adding one atom to the bottom of Nb_{22}, and by further adding an edge-capped atom, Nb_{24} is obtained.

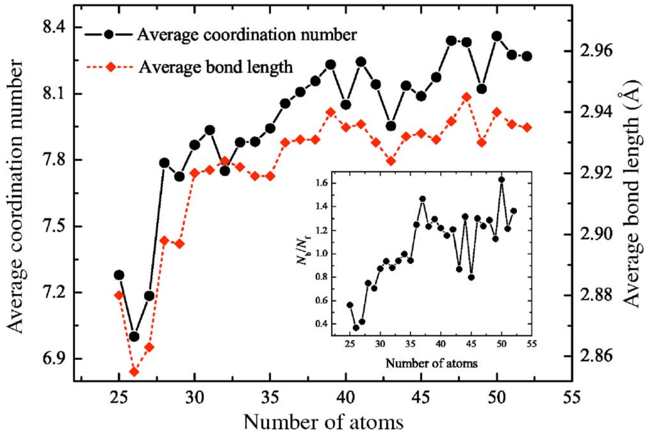

FIG. 2. (Color online) Average coordination number (average bond length) vs cluster size, guided for the eyes with solid and dashed lines, respectively. The inset shows the ratio of body atom number to surface atom one, denoted as N_b/N_f.

Now, we pay more attention to the larger Nb_N ($N=25$–52) by the same computational scheme. The obtained results suggest that they prefer the amorphous packing, making the compact oblate-spherical configurations dominant. The average coordination number and bond length as well as the ratio of body atom number to surface atom one (N_b/N_f) are shown in Fig. 2 for $25 \leqslant N \leqslant 52$. Here, the nearest-neighbor bond length is truncated at 3.3 Å, which is obtained by calculations of atom pair-correlation function $g(r)$ for all clusters. It can be seen clearly from Fig. 2 that both the average coordination number and bond length increase nonmonotonically with size, showing a close similarity to each other. The apparent size-dependent geometrical structures of Nb_N may play an important role in their physical properties. For example, the size-dependent deviation of the bond length from the bulk value may induce the symmetry breaking and so the emergence of EDM. It is also worth noticing that the dramatic even-odd oscillation behavior appears in N_b/N_f of Nb_N ($N \geqslant 40$), suggesting the growth pattern may be dualistic, which is different from even to odd Nb_N, leading to a probable even-odd variation of their physical properties.

Based upon the above structures, the second-order difference $\Delta_2\mathrm{E}(N)$ of BE varying with size is calculated and shown in the inset of Fig. 1, which evidently displays good agreement between both results from RECP and AESRC. The variation of $\Delta_2\mathrm{E}(N)$ shows that the magic number should emerge at $N=7$, 13, 15, 17, 22, 24, 27, 29, 31, 33, 35, 37, 41, 44, 47, and 50, which agrees well with the peaks in the abundant spectra of Nb_N at $N=7$, 13, 15, 22, 29, and 33.[21]

The extraordinary FE of Nb_N observed in the experiment[1] is particularly interesting. The calculated EDM curves are

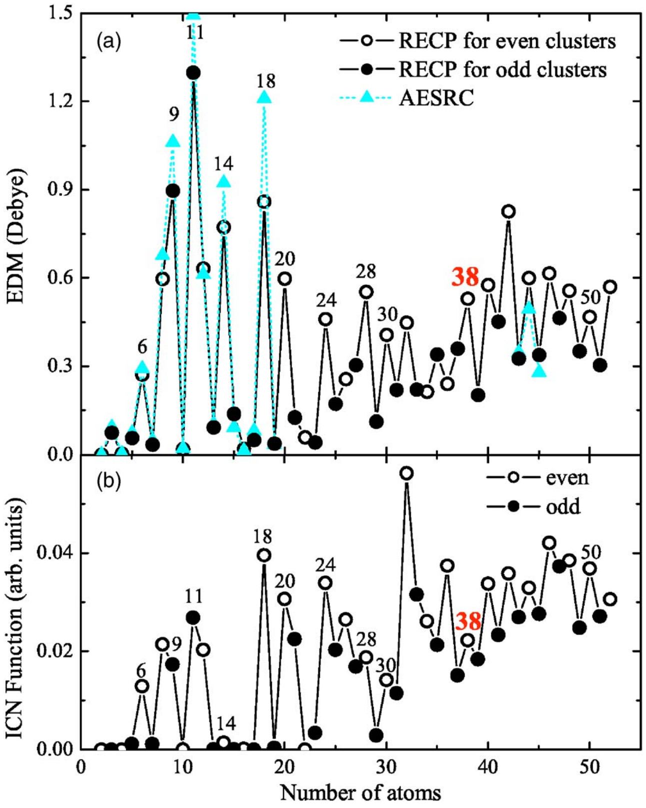

FIG. 3. (Color online) (a) DFT values of EDMs vs cluster size, calculated by two different methods, i.e., RECP (circles) and AESRC (triangle). (b) Dependence of the ICN function on cluster size. For clarity, the values of even and odd clusters are shown by open and filled circles, respectively.

shown in Fig. 3(a), from which we find again that the change of the RECP results agrees with that of the AESRC ones. In most cases, the RECP EDM values are smaller than the AESRC ones. However, the positions of local maximum and minimum EDMs obtained by RECP and AESRC are in good agreement with each other, which are also consistent with the experimental observations. For example, we obtained theoretically the local maximum EDMs at $N=14$, 18, 20, 24, and local minimum ones at $N=13$, 15, 19, 22 for the medium-size Nb_N ($N=13$–24). More importantly, a markedly even-odd EDM oscillation has been also reproduced theoretically, starting from Nb_{38}.

Obviously, the EDM of a niobium cluster is determined by its asymmetrical charge distribution (CD), which should be greatly influenced by its geometrical structure, such as its shape, surface atom number, and interatomic distances deviated from the bulk values, all of which induce a deformed CD. For example, the lowest-energy geometrical structure of Nb_6 is a distorted prism, which is more stable than the octahedron only by 0.03 eV. The approximate O_h symmetry of the latter prohibits the appearance of the EDM, while the former has an EDM of 0.2721 D due to inverse symmetry breaking. That is to say, the different isomers have different EDMs even if they are energetically close, showing also the geometrical structure of a niobium cluster has a very important effect on its EDM. With an increase of atoms, there exist some metastable isomers close to the lowest-energy structure in most of the Nb_N, whose EDM amplitudes may have a larger fluctuation. In order to detect further the isomer's effect on the EDM, we have given the results of some larger Nb_N in Table I, showing clearly the EDMs of different isomers fluctuate greatly. Typically, the variation of EDM between isomers, within a vibrational temperature of 100 K,[22] at a given size is about 0.3–0.9 D, which is obviously larger than the even-odd oscillation amplitude of EDMs between neighboring Nb_N (about 0.1–0.3 D). For example, the ground-state structure of Nb_{51} and its first close-lying isomer are close to each other in energy, but their EDMs differ heavily from each other, varying from 0.3020 D to 1.1736 D. As shown in Ref. 1, the electric deflection of Nb_N has been measured at finite temperatures, showing clearer even-odd oscillation starting from Nb_{38} at a lower temperature of 20 K. With temperature increasing, the oscillation amplitude becomes smaller and smaller, and finally disappears above 100 K. In our calculations, the isomer's influence on the EDM value plays also a "finite-temperature" effect. The better the structure optimization is, the clearer the even-odd oscillation behavior. In addition, we also found from Table I that the average coordination number of the ground-state structures is the largest in the isomers we considered, showing that the ground-state structures of Nb_N prefer compact configurations.

TABLE I. Relative energy, the EDM, and the average coordination number ($\bar{Z}$) of the ground state and its first two isomers of Nb_N at $N=38$–40, 50–52. The energetic differences between the isomers are at the limits of the accuracy of our DFT-GGA approach.

N	E (eV)	EDM (D)	$\bar{Z}$	N	E (eV)	EDM (D)	$\bar{Z}$
38a	0	**0.5290**	8.158	50a	0	**0.4677**	8.360
38b	0.074	0.3511	7.894	50b	0.203	0.4427	7.880
38c	0.268	0.2675	7.947	50c	0.452	0.5145	7.840
39a	0	**0.2018**	8.231	51a	0	**0.3040**	8.275
39b	0.072	0.4917	7.846	51b	0.025	1.1736	8.196
39c	0.184	0.5935	7.897	51c	0.163	1.1473	8.196
40a	0	**0.5758**	8.050	52a	0	**0.5696**	8.269
40b	0.176	0.2920	8.025	52b	0.142	0.8694	8.038
40c	0.257	0.5215	7.700	52c	0.325	0.3374	7.750

In order to further find what causes the anomalous EDMs of Nb_N, we have introduced the concept of effective charge to characterize the bonding variations in a cluster, which could be obtained by calculation of the coordination number because it can reflect, to some extent (although not very precisely), the size-dependent structures of Nb_N. Due to the inequivalent geometrical surroundings of each atom in a cluster, the electron density should not distribute uniformly between two nearby atoms forming a chemical bond, leading to different effective charges on the atoms of a Nb_N and so emergence of its EDM. It is obvious that the effective charge on an atom decreases with an increase of its coordination number, i.e., an atom with higher coordination number should possess less effective charge. Therefore, we adopt simply an inverse coordination number (ICN) as a weight index to quantify the effective CD in a Nb_N, which could be represented by a function $F(N)$, defined as

$$F(N) = \left| \frac{1}{B} \sum_{\substack{i,j=1 \\ r_{ij}<R_{cut}}}^{N} \frac{\vec{R}_i/Z_i + \vec{R}_j/Z_j}{1/Z_i + 1/Z_j} \right|,$$

where $B=\frac{1}{2}\sum_{i=1}^{N} Z_i$ is the total bonding number with Z_i the coordination number of the ith atom. R_{cut} is the cutoff distance (3.3 Å) and $\vec{R}_i$ is the position vector of the ith atom (the coordinate origin is set at the mass center of the cluster).

The $F(N)$ values of Nb_N (N=2–52) are shown in Fig. 3(b), which displays almost the same variation behavior as the EDMs, demonstrating that it correctly describes the CD deformation in Nb_N. For example, for the smaller Nb_N, the ICN function reproduces again the local maxima and minima of EDMs at N=6, 11, 18, 20, 24, 28, 30 and at N=4, 7, 10, 13, 15, 17, 19, 29, respectively. In particular, for the larger Nb_N with $N \geqslant 38$, the ICN values are enhanced for even clusters, but suppressed for odd ones, reproducing the extraordinary even-odd EDM oscillation shown in Fig. 3(a), which clearly indicates that the ICN function indeed can be used to characterize the effective CD in Nb_N qualitatively, although it is so simple and elegant.

The close relation between the Nb_N structures and their corresponding EDMs can also be identified by visualization of the spatially deformed CD in the clusters, which is defined as the total charge density minus the density of the isolated atoms. Thus, the regions with positive deformation charge density will indicate formation of the bonds, while the negative regions indicate electron loss. For example, the bonding characters of Nb_{19} and Nb_{20} with isodensity surface of value 0.05 e/a.u.^{3} are illustrated in Fig. 4, which clearly shows the difference between their deformation charge densities. A slightly distorted double-icosahedral structure of Nb_{19} induces its charge isocontour with an approximate D_{5h} symmetry, showing an almost zero EDM. However, the obviously different CD from top to bottom of Nb_{20} shown in Fig. 4(b) gives rise to its rather larger EDM, denoted by an arrow. So, we conclude at this point that the different structures of Nb_N will induce much different spatial CD, leading to different EDM values of Nb_N.

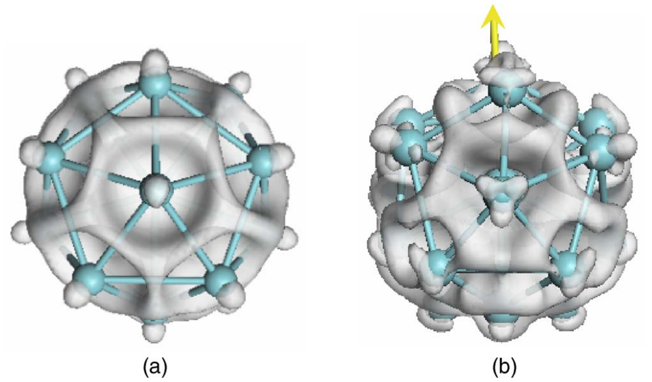
(a) (b)

FIG. 4. (Color online) The deformation densities for (a) Nb_{19} and (b) Nb_{20}, in which the direction of the EDM is denoted by the arrow. The isodensity surface corresponds to 0.05 e/a.u.^{3}.

IV. CONCLUSION

In summary, the equilibrium geometries, relative stabilities, and EDMs of Nb_N (N=2–52) have been calculated by a combination of the empirical interaction model and DFT optimization. More attention has been paid to the effects of the Nb_N structures on their EDMs. It is found that no one Nb_N mimics the bulk structure and the compact oblate-spherical amorphous structures are preferable for the larger Nb_N ($N \geqslant 25$). Interestingly, the size-dependent structures of Nb_N are found to be an intrinsic origin to induce their unordinary FE. Our study shows that the EDM does exist in most of the niobium clusters and has a close relationship with their geometrical structures. A simple ICN function is proposed to account for the anomalous size- and structure-dependent variations in the EDMs of Nb_N. Good agreement between the ICN function and the theoretical values of EDMs as well as the experiment demonstrates the geometrical structure of Nb_N has an important effect on its ferroelectric property.

ACKNOWLEDGMENTS

We acknowledge valuable discussions with Walt A. de Heer on his experimental results, and we also thank Professor V. Kumar and Y. Kawazoe for stimulating discussions. This work is supported by the Natural Science Foundation of China under Grant No. A040108, and also the State Key Program of China under Grant No. 2004CB619004. The DFT calculations were made on the SGI Origin-3800 and 2000 supercomputer.

*Corresponding author. Email address: jdong@nju.edu.cn

[1] R. Moro, X. Xu, S. Yin, and W. A. de Heer, Science **300**, 1265 (2003).

[2] M. B. Knickelbein, J. Chem. Phys. **118**, 6230 (2003).

[3] C. D. Batista, J. E. Gubernatis, J. Bonca, and H. Q. Lin, Phys. Rev. Lett. **92**, 187601 (2004).

[4] L. Goodwin and D. R. Salahub, Phys. Rev. A **47**, R774 (1993).

[5] H. Gronbeck and A. Rosen, Phys. Rev. B **54**, 1549 (1996); H. Gronbeck, A. Rosen, and W. Andreoni, Phys. Rev. A **58**, 4630 (1998).

[6] V. Kumar and Y. Kawazoe, Phys. Rev. B **65**, 125403 (2002).

[7] K. E. Andersen, V. Kumar, Y. Kawazoe, and W. E. Pickett, Phys. Rev. Lett. **93**, 246105 (2004).

[8] C. I. Chou and T. K. Lee, Acta Crystallogr., Sect. A: Found. Crystallogr. **58**, 42 (2001).

[9] C. I. Chou, R. S. Han, S. P. Li, and T. K. Lee, Phys. Rev. E **67**, 066704 (2003).

[10] V. N. Manoharan, M. T. Elsesser, and D. J. Pine, Science **301**, 483 (2003).

[11] M. W. Finnis and J. E. Sinclair, Philos. Mag. A **50**, 45 (1984).

[12] G. J. Ackland and R. Thetford, Philos. Mag. A **56**, 15 (1987).

[13] S. K. Nayak, B. K. Rao, S. N. Khanna, and P. Jena, Chem. Phys. Lett. **259**, 588 (1996).

[14] DMol3 is a density-functional-theory-based package with atomic basis, distributed by Accelrys [B. Delley, J. Chem. Phys. **92**, 508 (1990)].

[15] M. Dolg, U. Wedig, H. Stoll, and H. Preuss, J. Chem. Phys. **86**, 866 (1987).

[16] A. Bergner, M. Dolg, W. Kuechle, H. Stoll, and H. Preuss, Mol. Phys. **80**, 1431 (1993).

[17] J. P. Perdew, in *Electronic Structure of Solids '91*, edited by P. Ziesche and H. Eschrig (Akademie Verlag, Berlin, 1991); J. P. Perdew, J. A. Chevary, S. H. Vosko, K. A. Jackson, M. R. Pederson, D. J. Singh, and C. Fiolhais, Phys. Rev. B **46**, 6671 (1992).

[18] R. Fletcher, *Practical Methods of Optimization* (Wiley, New York, 1980), Vol. 1.

[19] For a niobium atom, the ionization potential and electron affinity obtained by RECP are 7.011 eV and 0.758 eV, respectively, which agree well with the experimental results: 6.76 eV and 0.89 eV. The calculated lattice parameter of 3.30 Å and cohesive energy of 7.26 eV per atom are also consistent with the experimental data of 3.30 Å and 7.57 eV/atom, respectively.

[20] The BE and bond length of Nb_2, obtained by RECP (AESRC), are 3.38 (4.88) eV and 2.18 (2.15) Å, respectively. The BE of AESRC agrees well with the experimental value of 4.86 ± 0.02 eV [M. D. Morse, Chem. Rev. (Washington, D.C.) **86**, 1049 (1986)], but that of RECP underestimates it. However, as we shall show, the structural and energetic features for Nb_N obtained by the two methods are in satisfactory agreement.

[21] M. Sakurai, K. Watanabe, K. Sumiyama, and K. Suzuki, J. Chem. Phys. **111**, 235 (1999).

[22] The vibrational temperature is calculated in terms of the energy difference by $T=2\Delta E/(3N-6)k_B$, where k_B is the Boltzmann constant.